Phase coherence in tight-binding models with nonrandom long-range hopping

D. B. Balagurov,[1,*] V. A. Malyshev,[2,3] and F. Domínguez Adame[4]
[1]*Scuola Normale Superiore and INFM, Piazza dei Cavalieri 7, 56126 Pisa, Italy*
[2]*S. I. Vavilov State Optical Institute, Birzhevaya Liniya 12, 199034 Saint Petersburg, Russia*
[3]*Institute for Theoretical Physics and Materials Science Center, University of Groningen, Nijenborgh 4, 9747 AG Groningen, The Netherlands*
[4]*GISC, Departamento de Física de Materiales, Universidad Complutense, E-28040 Madrid, Spain*
(Received 26 November 2003; published 25 March 2004)

The density of states, even for a perfectly ordered tight-binding model, can exhibit a tail-like feature at the top of the band, provided the hopping integral falls off in space slowly enough. We apply the coherent potential approximation to study the eigenstates of a tight-binding Hamiltonian with uncorrelated diagonal disorder and long-range hopping, falling off as a power μ of the intersite distance. For a certain interval of hopping-range exponent μ, we show that the phase-coherence length is infinite for the outermost state of the tail, irrespectively of the strength of disorder. Such an anomalous feature can be explained by the smallness of the phase-space volume for the disorder scattering from this state. As an application of the theory, we mention that ballistic regime can be realized for Frenkel excitons in two-dimensional molecular aggregates, affecting to a large extent the optical response and energy transport.

DOI: 10.1103/PhysRevB.69.104204 PACS number(s): 71.23.An, 78.40.Pg, 71.35.Aa

I. INTRODUCTION

The atomic orbital framework used to characterize electronic states in solids commonly deals with short-range hopping (SRH). For such situation it is well known that any disorder leads to randomization of the wave-function phase on some finite spatial scale known as phase-coherence length (PCL). Beyond this scale, roughly equal to the mean free path, the charge transport has a diffusive form until the coherent backscattering causes Anderson localization.[1] The nature of states to be localized or extended is governed by the dimensionality of the system.[2] Extensive studies have been carried out to establish the validity limits of the statement that all states in one-dimensional (1D) tight-binding models are localized, originally formulated for the case of diagonal uncorrelated disorder and SRH.[3] Recently, the absence of extended states in low-dimensional systems was questioned in Refs. 4–7 for *uncorrelated diagonal disorder* and nonrandom long-range hopping (LRH) falling off as some power of the intersite distance. To be specific, the authors considered the model Hamiltonian

$$H=\sum_{\mathbf{n}} \varepsilon_{\mathbf{n}}|\mathbf{n}\rangle\langle\mathbf{n}|+\sum_{\mathbf{n},\mathbf{m}} J_{\mathbf{nm}}|\mathbf{n}\rangle\langle\mathbf{m}|, \tag{1}$$

where $J_{\mathbf{nm}}=1/|\mathbf{n}-\mathbf{m}|^{\mu}$, and $\varepsilon_{\mathbf{n}}$ are uncorrelated random variables distributed according to the same distribution function $p(\varepsilon_{\mathbf{n}})$. (Energy is measured in units of the nearest-neighbor hopping.) The size scaling of the inverse participation ratio was investigated both numerically and with the use of supersymmetric method for disorder averaging combined with the renormalization group. The outcome indicated that for a d-dimensional lattice ($d=1,2$), provided $d<\mu<3d/2$, the uppermost states were subjected to the Anderson localization-delocalization transition with respect to the disorder magnitude, remaining delocalized for not very strong disorder. Such anomalous occurrence of extended states dramatically differs from what has been observed so far in the majority of localization problems.

The inverse participation ratio criterion, even though being a robust way to detect the Anderson localization, does not completely capture the underlying structure of the wave functions. In particular, such criterion does not seem to distinguish the case of pure Anderson transition from that in which the Anderson transition is accompanied by a transition from the diffusive to the ballistic regime. The realization of the second scenario would imply that not only the localization length, but also the PCL becomes infinite at the transition point. To best of our knowledge the PCL has never been addressed so far for LRH models. At the same time the physics of the diffusive-ballistic transition is much simpler than that of the localization transition since it deals essentially with the single-particle Green's function averaged over disorder realizations.

The aim of the present paper is to investigate the single-particle properties of the Hamiltonian (1). In particular, we demonstrate that in the interval of μ, coinciding with that reported in Ref. 6 for the existence of extended states, the PCL diverges at the upper band edge, even at moderate degree of disorder. The task is fulfilled by making use of the coherent-potential approximation (CPA), known to be the best available self-consistent approximation for the single-particle Green's function.[8] The paper is organized as follows. In Sec. II we present some preliminary considerations of the disorder-free system, which are necessary for a better understanding of the present paper. The body of the paper is Sec. III, where we present the CPA approach to study the single-particle Green's function averaged over disorder realizations. In particular, we discuss in detail its weak-disorder asymptotic solution. Then we proceed on to physical quantities such as band edge, spectral density, density of states (DOS), and PCL. The results of numerical simulations are summarized in Sec. IV, where we compare them to the ana-

lytical predictions of the preceding section. We conclude with a brief discussion of the relevance of the obtained results in Sec. V.

II. DISORDER-FREE SYSTEM

Without disorder ($\varepsilon_{\mathbf{n}}=0$) the eigenstates of Hamiltonian (1) are plane waves with quasimomenta $\mathbf{k}$ within the first Brillouin zone. The corresponding eigenenergies are given by

$$E_{\mathbf{k}}=\sum_{\mathbf{n}\neq\mathbf{0}}\frac{e^{i\mathbf{k}\cdot\mathbf{n}}}{|\mathbf{n}|^{\mu}}, \tag{2}$$

where summation runs over sites of a regular d-dimensional lattice ($d=1,2$). The lattice constant is set to unity. To deal with a bounded spectrum we assume $\mu>d$ throughout the paper. The complete account for all terms in the sum (2) is important in the neighborhood of the upper band edge, where the LRH strongly modifies the dispersion. Specifically, around $\mathbf{k}=\mathbf{0}$ the dispersion relation (2) is approximately as follows:

$$E_{\mathbf{k}}=E_0-A_d(\mu)|\mathbf{k}|^{\mu-d}-B_d(\mu)|\mathbf{k}|^2+O(|\mathbf{k}|^4). \tag{3}$$

Here, $E_0, A_d(\mu), B_d(\mu)$ are known positive constants.[5,6] Provided $\mu<d+2$, the second essentially nonquadratic term in Eq. (3) dominates for small $|\mathbf{k}|$ over the next quadratic term, and vice versa. We therefore cast expansion (3) in a shorthand form

$$E_{\mathbf{k}}=E_0-C_d(\mu)|\mathbf{k}|^{\nu_d(\mu)}, \tag{4}$$

where

$$C_d(\mu)=A_d(\mu),\quad \nu_d(\mu)=\mu-d \quad \text{for} \quad \mu<d+2,$$

$$C_d(\mu)=B_d(\mu),\quad \nu_d(\mu)=2 \quad \text{for} \quad \mu>d+2. \tag{5}$$

Straightforward calculation of the DOS in the vicinity of the upper band edge yields a power-law behavior

$$\rho(\omega)\sim a_d(\mu)|\omega-E_0|^{d/\nu_d(\mu)-1}. \tag{6a}$$

Here, the constant factor $a_d(\mu)$ is given by

$$a_d(\mu)=\frac{S_d}{(2\pi)^d}\frac{[C_d(\mu)]^{-d/\nu_d(\mu)}}{\nu_d(\mu)}, \tag{6b}$$

with S_d being the area of the d-dimensional unit sphere (we set $S_1=2$). It should be noticed that the DOS (6a) is very sensitive to the value of μ: the exponent $d/\nu_d(\mu)-1$ in Eq. (6a) has the familiar Van Hove form $(d-2)/2$ for $\mu>d+2$ and the less usual one, involving the dependence on μ, for the opposite inequality. Furthermore, as $\mu<3d/2$, both the DOS and its derivative vanish at the energy E_0, indicating that this part of the energy spectrum is weakly populated by the states. In spite of a qualitative resemblance of a disorder-induced band tail, in the model under consideration this is a purely kinetic feature, stemming from the long-range nature of hopping.

Besides the unusual form of the DOS, the LRH results not in exponential but rather a power-law localization of states. Previously found in numerical simulations,[9] this feature can be easily understood considering a nontypical site energy fluctuation, i.e., the one with site energy $\varepsilon_{\mathbf{n}}$ essentially outside of the band. Then, the first order of perturbation theory with respect to the off-diagonal part of the Hamiltonian (1) yields the corresponding wave function $\Phi_{\mathbf{nm}}=\delta_{\mathbf{nm}}+J_{\mathbf{nm}}/\varepsilon_{\mathbf{n}}$ which falls off as $1/|\mathbf{n}-\mathbf{m}|^{\mu}$ upon increasing the distance from the site $\mathbf{n}$. Remarkably, $\Phi_{\mathbf{nm}}$ does not vanish outside some finite real-space interval, as it would be for a perturbative wave function in the case of SRH. This means that for the LRH the perturbation theory provides an approximate solution valid in all space, and no higher-order corrections are needed as long as $|\varepsilon_{\mathbf{n}}|\gg|J_{\mathbf{nm}}|$. For a generic relation between $\varepsilon_{\mathbf{n}}$ and $J_{\mathbf{nm}}$ the omitted orders will correct the coefficient of the $1/|\mathbf{n}-\mathbf{m}|^{\mu}$ dependence and introduce some new terms falling off faster than $1/|\mathbf{n}-\mathbf{m}|^{\mu}$. For $\varepsilon_{\mathbf{n}}$ inside the band, both power-law and exponentially falling-off components in the wave function will appear. Their form can be deduced from calculations presented in the Appendix for the case of 1D system.

III. COHERENT-POTENTIAL APPROXIMATION

The CPA is a reliable and efficient method to study the disorder-averaged DOS and the phase coherence between wave functions for different members of the random ensemble.[8,10] These characteristics can be extracted from the disorder-averaged single-particle propagator

$$G(\omega)=\int\prod_{\mathbf{n}}d\varepsilon_{\mathbf{n}}p(\varepsilon_{\mathbf{n}})\frac{1}{\omega-H}. \tag{7}$$

Unless otherwise specified, the energy variable ω will have an infinitesimal positive imaginary part. In the framework of CPA, quantity (7) is approximated in a self-consistent way to preserve its analytic properties and deliver the correct limiting behavior as either the disorder strength or the hopping amplitude tends to zero. Namely, it is argued that a good approximation for the single-particle propagator is to treat its disorder-generated self-energy as a site-diagonal quantity. In other words, average (7) is evaluated by replacing the site energy $\varepsilon_{\mathbf{n}}$ by a coherent potential $\sigma(\omega)$,

$$G_{\mathbf{k}}(\omega)=\frac{1}{\omega-\sigma(\omega)-E_{\mathbf{k}}}. \tag{8}$$

The choice of $\sigma(\omega)$ should be such to compensate on average scattering from a single site. The resulting self-consistency condition reads (see, e.g., Ref. 10)

$$\int d\varepsilon_{\mathbf{n}}p(\varepsilon_{\mathbf{n}})\frac{\varepsilon_{\mathbf{n}}-\sigma(\omega)}{1-[\varepsilon_{\mathbf{n}}-\sigma(\omega)]G_{\mathbf{nn}}(\omega)}=0, \tag{9}$$

where $G_{\mathbf{nn}}(\omega)$ is the site-diagonal element of the CPA Green's function.

We adopt for the random site energies the distribution uniform within symmetric interval $[-\Delta,\Delta]$. For such

$p(\varepsilon_{\mathbf{n}})$, the integral in Eq. (9) can be evaluated explicitly, and we get the self-consistency equation in the form

$$\frac{1}{2\Delta}\ln\frac{1+[\sigma(\omega)+\Delta]G_{\mathbf{nn}}(\omega)}{1+[\sigma(\omega)-\Delta]G_{\mathbf{nn}}(\omega)}=G_{\mathbf{nn}}(\omega). \tag{10}$$

The resulting CPA propagator will be studied numerically in Sec. IV. In the rest of the present section, we derive an analytic solution of the theory in the weak-disorder limit. As an outcome, the asymptotic formulas for the observable quantities, namely band-edge energy, spectral density, DOS, and PCL, will be obtained.

A. Weak-disorder self-energy

To access the weak-disorder limit of CPA we perform a formal small-Δ expansion in Eq. (10) retaining terms up to Δ^2. Then the self-consistency condition acquires the form

$$\sigma(\omega)=\frac{\Delta^2}{3}\frac{G_{\mathbf{nn}}(\omega)}{[1+G_{\mathbf{nn}}(\omega)\sigma(\omega)]^2}. \tag{11}$$

The term $G_{\mathbf{nn}}(\omega)\sigma(\omega)$ in the denominator can be neglected because eventually it turns out to be proportional to a positive power of $\Delta\ll 1$. Thus the weak-disorder equation to be analyzed reads

$$\sigma(\omega)=\frac{\Delta^2}{3}G_{\mathbf{nn}}(\omega). \tag{12}$$

Both of the two approximative steps yielding Eq. (12) do not introduce any spurious singularities around the band edges, e.g., such as those emerging after truncation of the cumulant series for the Green's function (see Ref. 10). Such preservation of the analyticity in the vicinity of the band edge is guaranteed by the full account for self-energy in the local Green's function entering the equation. We notice that the coefficient $(1/3)\Delta^2$ in Eq. (12) coincides with the site-energy variance, the second centered moment of $p(\varepsilon_{\mathbf{n}})$. From this remark, we conclude that the weak-disorder equation (12) holds for any distribution function $p(\varepsilon_{\mathbf{n}})$ decreasing fast enough at large $\varepsilon_{\mathbf{n}}$ (specifically, if the Mth-order centered moment scales as Δ^M).

Weak disorder mixes only a small part of otherwise well-defined-momenta states within an energy interval of the order of the effective broadening $\sim \mathrm{Im}\,\sigma(\omega)$. This facilitates evaluation of the site-diagonal propagator entering Eq. (12). Namely, for energies close to the upper band edge only small $\mathbf{k}$ will contribute to $G_{\mathbf{nn}}(\omega)=\Sigma_{\mathbf{k}}G_{\mathbf{k}}(\omega)$. Because $\sigma(\omega)$ is small due to the weakness of disorder, while the detuning $\omega-E_0$ can be made small close enough to the upper band edge, the site-diagonal Green's function can be found as

$$G_{\mathbf{nn}}(\omega)\sim\frac{\pi a_d(\mu)[\omega-E_0-\sigma(\omega)]^{d/\nu_d(\mu)-1}}{\sin[\pi d/\nu_d(\mu)]}+b_d(\mu). \tag{13}$$

Here, the first term [in which $a_d(\mu)$ is given by Eq. (6b)] comes solely from the small momenta and does not depend on any momentum cutoff. The magnitude of the contributing $\mathbf{k}$ can be estimated from the dispersion law (4) as $k\sim|\omega-E_0-\sigma(\omega)|^{1/\nu_d(\mu)}$. The imaginary part of the considered term is nonzero in the limit of vanishing disorder $[\sigma(\omega)=0]$, in agreement with the singular or tail-like DOS of Eq. (6a). The second term in Eq. (13) is a *real* constant representing the part of the site-diagonal propagator whose dependence on energy is smooth near the upper band edge; the major contribution comes from the higher $\mathbf{k}$. The exact value of $b_d(\mu)$ can be found via numerical summation over all momenta in $G_{\mathbf{nn}}(\omega)$.

Accounting for the constant $b_d(\mu)$ in the weak-disorder self-consistency equation (12) is equivalent to a shift of both the band-edge position and the self-energy. Namely, upon transformation $E_0'=E_0+(1/3)\Delta^2 b_d(\mu)$, $\sigma'(\omega)=\sigma(\omega)-(1/3)\Delta^2 b_d(\mu)$, Eq. (12) takes a form as if only the low-momenta states were participating in the disorder scattering:

$$\sigma'(\omega)=\frac{\Delta^2}{3}\frac{\pi a_d(\mu)[\omega-E_0'-\sigma'(\omega)]^{d/\nu_d(\mu)-1}}{\sin[\pi d/\nu_d(\mu)]}. \tag{14}$$

While $E_0'-E_0$ is a mere shift the uppermost states acquire due to the coupling to the continuum of remote low-energy (high-momenta) states, the broadening effect, accounted through Eq. (14), originates from the mixing of nearby states at the band edge.

The solution of Eq. (14) turns out to be extremely sensitive to the value of the exponent μ. In particular, for a fixed energy $\omega=E_0'$ it follows that either

$$\sigma'(E_0')=\left\{\frac{\Delta^2}{3}\frac{\pi a_d(\mu)}{\sin[\pi d/\nu_d(\mu)]}\right\}^{\nu_d(\mu)/[2\nu_d(\mu)-d]} \tag{15a}$$

or

$$\sigma'(E_0')=0. \tag{15b}$$

The former expression can be considered as being valid only at $\mu>3d/2$ where $\nu_d(\mu)>d/2$, because otherwise (at $\mu<3d/2$) the exponent $\nu_d(\mu)/[2\nu_d(\mu)-d]$ becomes negative, resulting in failure of the zero-disorder limit. Then, the latter expression should be used.

From the presented arguments it follows that the renormalized self-energy remains finite at $\omega=E_0'$ varying with energy on the scale $\sim\Delta^{2\nu_d(\mu)/[2\nu_d(\mu)-d]}$ provided $\mu>3d/2$. The complete solution of Eq. (14) in this case looks rather involved, but for the forthcoming, qualitative considerations based on disorder scaling

$$\sigma'(\omega)\sim\Delta^{2\nu_d(\mu)/[2\nu_d(\mu)-d]} \tag{16a}$$

will suffice. Regarding the range of $\mu<3d/2$, the renormalized self-energy vanishes faster than linearly as ω approaches E_0'. The solution in this case can be obtained in a closed form

$$\sigma'(\omega)\sim\frac{\Delta^2}{3}\frac{\pi a_d(\mu)}{\sin[\pi d/\nu_d(\mu)]}(\omega-E_0')^{d/\nu_d(\mu)-1}. \tag{16b}$$

Having derived the CPA self-energy, at next step we present analytical results concerning observable quantities, namely band-edge energy, spectral density, DOS, and PCL.

B. Band-edge energy

The CPA band edge, denoted by $\tilde{E}$, is determined as the maximum energy at which $\mathrm{Im}\sigma(\omega)\neq 0$. As follows from the above considerations, $\tilde{E}$ is shifted from its disorder-free value E_0, first, by $(1/3)\Delta^2 b_d(\mu)$ due to scattering processes involving large $\mathbf{k}$ states, and second, by an amount $\sim\Delta^{2\nu_d(\mu)/[2\nu_d(\mu)-d]}$ giving the scale on which the renormalized self-energy varies significantly. Comparing the disorder scaling exponent appearing in the two contributions, we conclude that the former prevails over the latter provided $\nu_d(\mu)>d$. Since it is always $\nu_d(\mu)\leqslant 2$ in 2D systems, the disorder-induced shift $\tilde{E}-E_0$ scales as Δ^2. In 1D system the scaling depends on the hopping exponent: for $\mu<2$ one gets $\tilde{E}-E_0\sim\Delta^2$, while $\tilde{E}-E_0\sim\Delta^{2(\mu-1)/(2\mu-3)}$ for $\mu>2$.

C. Spectral density

Along with the results reported in Sec. III A, one can also obtain the disorder-averaged spectral density at the upper band edge:

$$A_{\mathbf{k}}(\omega)=-\frac{1}{\pi}\,\mathrm{Im}\;G_{\mathbf{k}}(\omega). \tag{17}$$

From Eq. (8) the energy-domain width of the spectral density can be estimated as $\gamma\sim|\mathrm{Im}\;\sigma(\omega)|$. As has been demonstrated above, if the LRH exponent μ is greater than $3d/2$, such width will scale upon disorder as

$$\gamma\sim\Delta^{2\nu_d(\mu)/[2\nu_d(\mu)-d]}. \tag{18}$$

This formula is a generalization of the disorder-induced linewidth estimate $\gamma\sim\Delta^{4/3}$ known for 1D tight-binding models with SRH.[11,12] Upon increasing the hopping range (decreasing μ) the disorder broadening of the resonance becomes less pronounced. As μ goes below $3d/2$, the zero-momentum spectral density acquires a power-law form

$$A_{\mathbf{k}=0}(\omega)\sim\Delta^2|\omega-E_0'|^{d/\nu_d(\mu)-3}. \tag{19}$$

Noticeably, for the specified interval of μ the exponent $d/\nu_d(\mu)-3$ is greater than -1. This guarantees integrability of the spectral density around $\omega=E_0'$. Hence, there is no contradiction with the single-particle sum rule.

D. Density of states

The next important question we address is the asymptotic behavior of the DOS in the proximity of the band edge. Expression (13) can be used to relate the DOS

$$\rho(\omega)=-\frac{1}{\pi}\,\mathrm{Im}\;G_{\mathbf{nn}}(\omega) \tag{20}$$

to the CPA self-energy. As follows from Eq. (12), the DOS drops abruptly, i.e., has infinite derivative at the band edge, provided $\mu>3d/2$. In the opposite case, $\mu<3d/2$, using Eq. (16b) we obtain

$$\rho(\omega)\sim a_d(\mu)|\omega-E_0'|^{d/\nu_d(\mu)-1}. \tag{21}$$

Here, the DOS profile remains similar to that of the nondisordered system [Eq. (6a)], the only difference being the band-edge location.

E. Phase coherence length

The PCL, to be denoted by $N(\omega)$, is usually defined as the inverse exponent responsible for exponential falloff of the coordinate-space single-particle propagator.[13] Such definition cannot be straightforwardly adopted in the case of LRH because, as demonstrated in the Appendix, the propagator falls off in essentially nonexponential way. Instead, we shall relate the PCL to an appropriately measured momentum-domain width of the spectral function $\kappa(\omega)$, through $N(\omega)=1/\kappa(\omega)$. For energies close to the upper band edge, $\kappa(\omega)$ is estimated from Eqs. (4) and (8) to be

$$\kappa(\omega)\sim\ \mathrm{Im}\left[-\frac{\omega-E_0-\sigma(\omega)}{C_d(\mu)}\right]^{1/\nu_d(\mu)}. \tag{22a}$$

Using Eq. (16a) for the CPA self-energy, one gets the following disorder scaling of the PCL valid in the range $\mu>3d/2$:

$$N(\omega)\sim\Delta^{-2/[2\nu_d(\mu)-d]}. \tag{22b}$$

It is worth noticing that scaling (22b) is nicely reproduced by means of a simple argument similar to that used in Ref. 12 for the SRH model. One proceeds confronting the two quantities:[12] energy spacing δE between two adjacent states localized within domain of a linear size N, and the reduced disorder magnitude $\sim\Delta N^{-d/2}$ seen by the localized quasiparticle, the effect known as exchange narrowing.[14] Using value N as a quantization length, from Eq. (4) we can estimate the energy spacing $\delta E\sim N^{-\nu_d(\mu)}$. Applying condition $\delta E\sim\Delta N^{-d/2}$, one arrives at the disorder scaling of N as is given in Eq. (22b). Furthermore, the spectral density width (18) is recovered being identified with the exchange-narrowed disorder magnitude $\sim\Delta N^{-d/2}$ where N is found above.

For $\mu<3d/2$, special attention should be paid on the fact that $\sigma'(\omega)$ vanishes faster than linearly as ω approaches E_0'. Direct calculation shows that in this case, the PCL inside the spectral region ($\omega<E_0'$) scales as

$$N(\omega)\sim\frac{1}{\Delta^2}|\omega-E_0'|^{2-(d+1)/\nu_d(\mu)}. \tag{22c}$$

Remarkably, such $N(\omega)$ diverges not only upon decreasing the strength of disorder Δ, but also as energy ω approaches the band edge. From both Eqs. (22b) and (22c) it follows that the PCL is infinite at the upper band edge in the marginal case $\mu=3d/2$.

IV. NUMERICAL RESULTS

To further clarify the properties possessed by the LRH model (1), we solved the CPA equations numerically, without any of approximations used in the above analytical treatment. In this section, we present the numerical results and compare them to those obtained in Sec. III. The self-

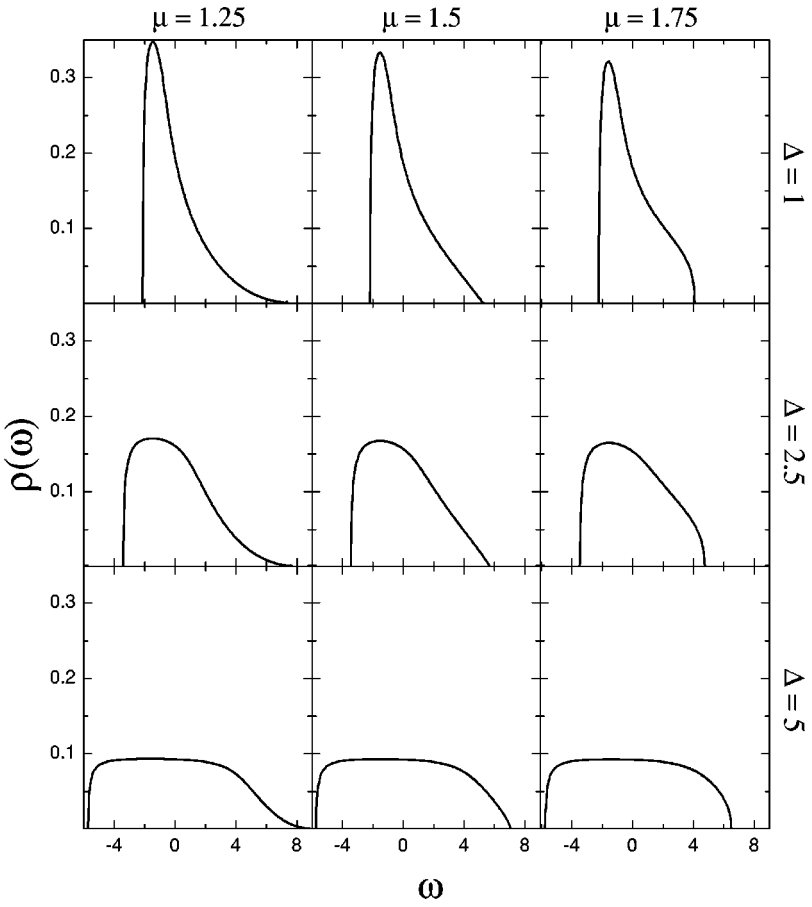

FIG. 1. CPA DOS calculated for several values of disorder strength Δ and hopping-range exponents μ.

consistency equation (10) was solved using a standard iterative scheme; the momentum integral $G_{\mathbf{nn}}(\omega)=\Sigma_{\mathbf{k}}G_{\mathbf{k}}(\omega)$ was evaluated with an efficient mesh-optimized algorithm. For definiteness, we restricted ourselves to one dimension, $d=1$. To check the accuracy of CPA, we also directly diagonalized the Hamiltonian (1) for an open chain of $\mathcal{N}=1000$ sites with statistical averaging over 500 disorder realizations.

The calculated DOS profiles are presented in Fig. 1 for $\mu=1.25$, $\mu=1.5$ (marginal case), and $\mu=1.75$, and several values of the disorder strength. We notice difference in the behavior of the CPA DOS at the high-energy tail depending on the exponent μ, in accordance with the previous discussion. We also observe that the low-energy side of the DOS is almost independent of μ since the dispersion relation of the disorder-free system is parabolic at the bottom of the band.[6] As illustrated in Fig. 2, even for noticeable disorder ($\Delta=2.5$) the CPA is in excellent agreement with the exact diagonalization. Such impressive accuracy of CPA for tight-binding models with simple band structure is guaranteed by the high number of energy-domain moments of the spectral density being reproduced exactly.[15] At the same time, the fully numerical spectrum suffers from finite-size oscillations, especially noticeable in the DOS tail for values of μ close to unity. The lack of smoothness is an unavoidable consequence of the smallness of DOS in this spectral region. To estimate the finite-size contribution one can look at spacing δE between the ground and the first size-quantization levels with the disorder being turned off. As follows from Eq. (4), such spacing scales with length $\mathcal{N}$ of the chain as $\delta E\sim\mathcal{N}^{1-\mu}$. The hopping integral falling off slowly enough ($\mu-1\ll 1$) leads to the rapidly growing size of matrices needed to avoid the discreteness of DOS in the tail region. For instance, to get a reasonably small value $\delta E=0.01$ for $\mu=1.25$, one would have to handle numerically the matrices of rather generic structure with size $\mathcal{N}\sim 10^8$, the task unaffordable for computers.

To check the analytic expression (21) against the full CPA solution we plotted in Fig. 3 a power of the CPA DOS with the exponent equal to the inverse of that in formula (21) with $d=1$. The fact that all curves with μ not exceeding 3/2 can be fitted to a straight line near the upper band edge confirms the validity of the asymptotic (21). The shift of the upper band edge with respect to its disorder-free location can be

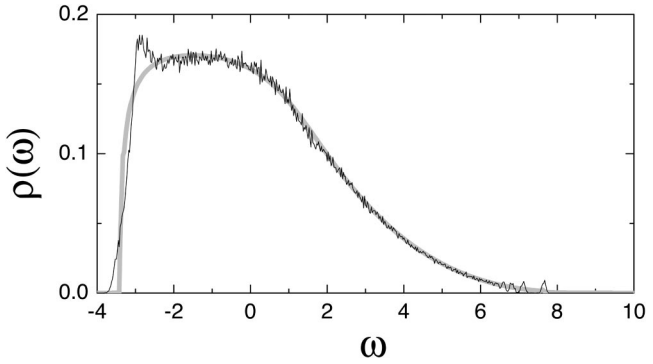

FIG. 2. CPA DOS (bold line) compared to that of exact diagonalization (narrow line) for $\mu=1.25$ and $\Delta=2.5$.

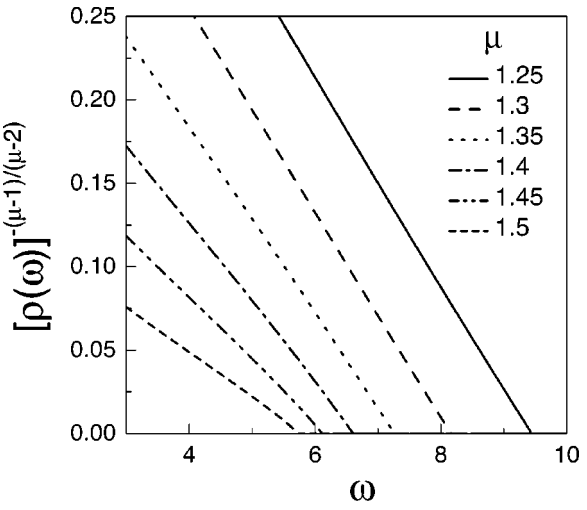

FIG. 3. CPA DOS after the power transformation. The degree of disorder Δ is 2.5 for all curves.

extracted from the data presented in Fig. 3. The CPA results concerning the band edge are summarized in Fig. 4. The figure illustrates the general tendency of the band edge to become more sensitive to disorder with increasing the range of hopping. We also verified the scaling arguments of Sec. III B concerning the band edge by fitting the displacement $\tilde{E}-E_0$ to a power law of Δ. The outcome, summarized in the inset of Fig. 4, demonstrates a qualitative agreement between the weak-disorder analytical considerations and the full CPA solution. The agreement is especially good in the extreme limits of very large and very small range of hopping ($\mu-1 \ll 1$ and $\mu > 3$, respectively). The discrepancy in the intermediate region is caused by an insufficient precision while separating out the dominating power-law contribution in the presence of other similar contributions with close exponents.

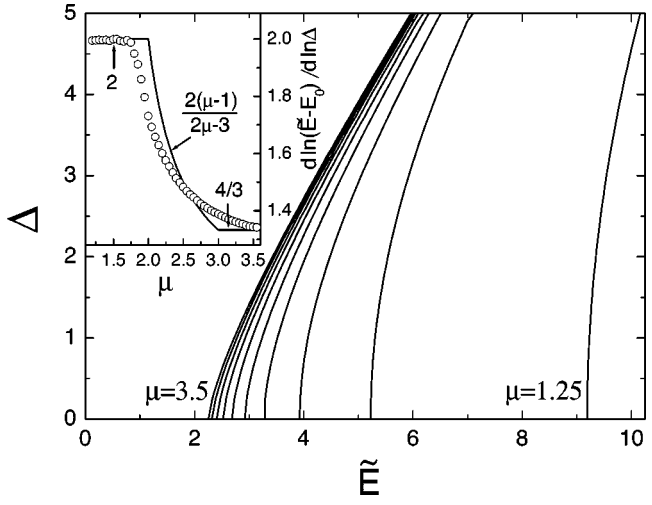

FIG. 4. Dependence of the CPA upper band edge on the degree of disorder. Curves are plotted for several fixed μ selected between 1.25 and 3.5 with step 0.25. The open circles in the inset show the exponent obtained after fitting $\tilde{E}-E_0$ with a power-law function of disorder. The same exponent predicted by the weak-disorder analytic solution is shown with solid line.

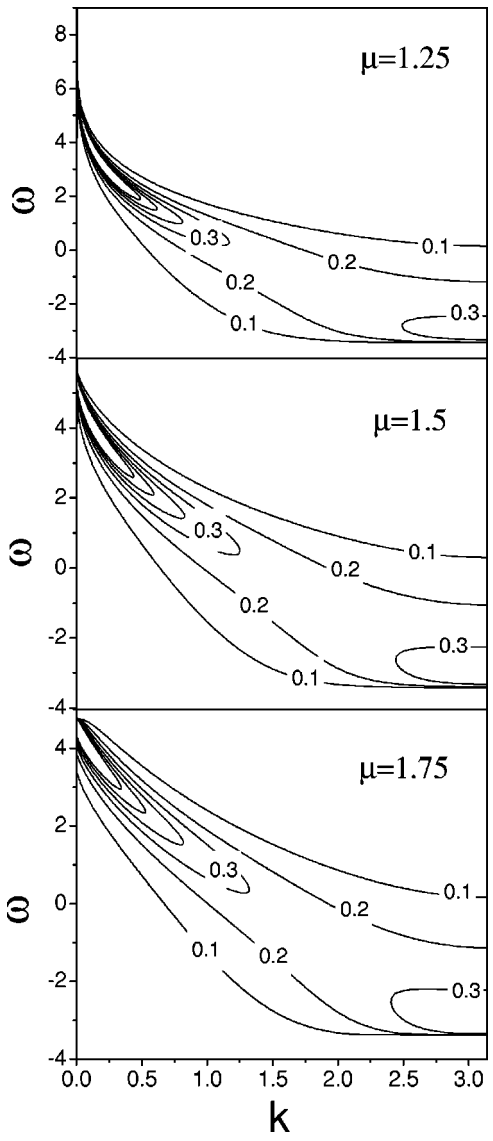

FIG. 5. Contour plots of the CPA spectral density $A_{\mathbf{k}}(\omega)$ for $\mu = 1.25, 1.5, 1.75$ and degree of disorder $\Delta = 2.5$.

So far, we were using the information contained in the site-diagonal part of the Green's function. Now we turn to the off-diagonal part of $G(\omega)$ to reveal physics which is related to the PCL. In Sec. III E it has been anticipated that the PCL behaves in an essentially different way in the two ranges of the hopping exponent μ separated by $\mu = 3/2$ (marginal case): it remains finite across the band as $\mu > 3/2$ while having a power-law singularity at the upper band edge as $\mu < 3/2$. To illustrate the argumentation used, we plot in Fig. 5 the momentum-domain spectral density obtained within the CPA for three values of μ: $\mu < 3/2$, $\mu = 3/2$, and $\mu > 3/2$. The first plot ($\mu = 1.25$) clearly shows that the width of the resonance along the momentum axis vanishes as the energy approaches the upper band edge. In contrast, the same width remains finite for $\mu = 1.75$. The observed behavior is in complete agreement with the general definition (22a) and the asymptotic formulas for the PCL presented in Sec. III E.

With the same values of μ as above we also computed the real-space spectral density $A_{\mathbf{nm}}(\omega)$ for several fixed energies.

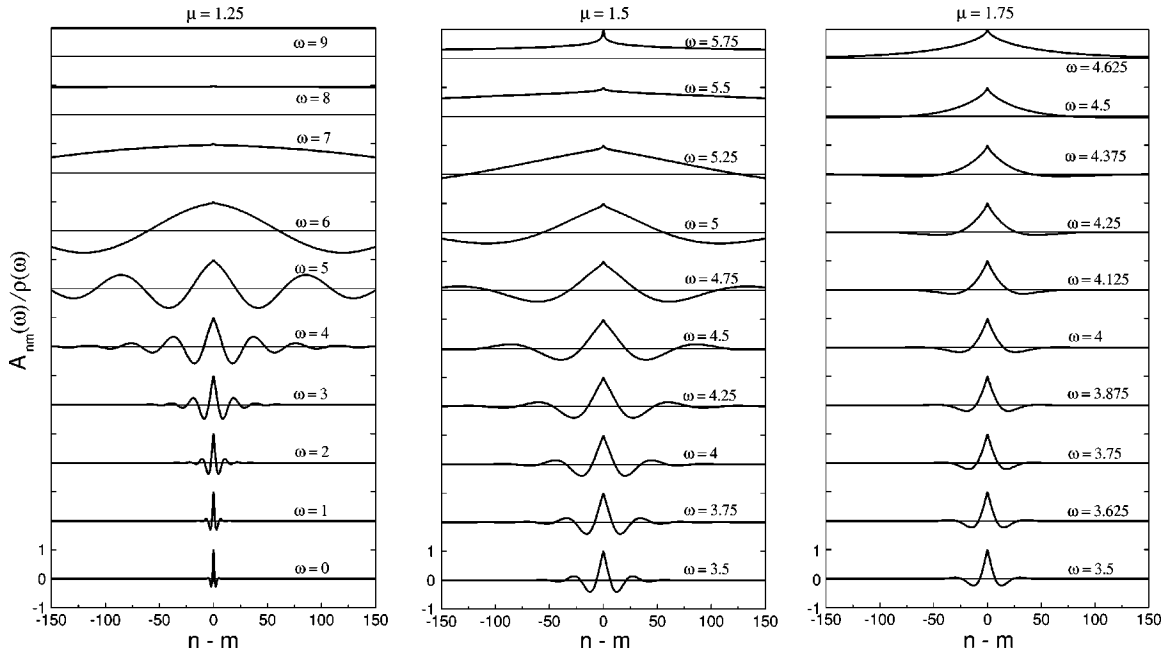

FIG. 6. Real-space spectral density normalized to the DOS. The degree of disorder Δ is 2.5 for all curves.

The quantity plotted in Fig. 6 is the real-space spectral density normalized to the DOS: it is unity when taken about the same site $[\rho(\omega)=A_{\mathbf{nn}}(\omega)]$. For energies located sufficiently far from the upper band edge, $A_{\mathbf{nm}}(\omega)$ displays damped oscillations as a function of the distance between sites. Their periodicity is approximately determined by the disorder-free momentum at the specified energy; naturally, it decreases upon approaching the upper band edge that in the absence of disorder would correspond to zero momentum. The inverse damping rate of the oscillations provides an estimate of the PCL.

Before discussing PCL in more detail, let us make some remarks on the spatial behavior of the Green's function. As it was first mentioned in Sec. II, the real-space Green's function contains not only a contribution varying exponentially with coordinate, but also one falling off according to a power law. In 1D system with arbitrary disorder-induced self-energy, the main power-law contribution is given by Eq. (A3). The best way to illustrate the presence of such power-law component is to plot the product $|\mathbf{n}-\mathbf{m}|^{\mu}A_{\mathbf{nm}}(\omega)$ against the coordinate, as is done in Fig. 7. The finite offset of the plotted quantity for large $|\mathbf{n}-\mathbf{m}|$ is in good agreement with that following from the asymptotic expression (A3).

The magnitude of the Green's-function component falling off exponentially with coordinate is determined by the complex roots k of the equation $E_k=\omega-\sigma(\omega)$. Typical trajectories of $k(\omega)$ for varying energy are shown in Fig. 8. For concreteness, only the solutions with negative imaginary part were considered. The roots exist only for ω below some critical energy $\overline{E}$. As ω reaches $\overline{E}$, the root disappears encountering the branch cut of the multivalued function E_k running along the imaginary axis. Hence the exponential contribution vanishes for all ω above the critical energy. In order to elucidate whether the energies $\omega>\overline{E}$ still belong to the spectrum we plotted in the inset to Fig. 8 the critical energy against the upper band edge for different exponents μ. As follows from this plot, for $\mu<3/2$ the energy $\overline{E}$ coincides with $\tilde{E}$, i.e., the exponentially falling-off component of the Green's function exists for all ω up to the band edge. Furthermore, as can be seen in Fig. 8, for the above indicated interval of μ, Im $k(\omega)$ vanishes at $\omega=\tilde{E}$. Hence, the exponential component of the Green's function will have constant envelope at the upper band edge, thereby extending infinitely in space. This behavior is indeed observed in the panel of Fig. 6 with $\mu=1.25$, thus confirming the main statement of the paper about the divergence of the PCL. Regarding the interval $\mu>3/2$, it follows from the inset of Fig. 8 that the energy $\overline{E}$ lies inside the band. In this case, the PCL remains finite across the band as is illustrated in Fig. 6 (panel of $\mu=1.75$).

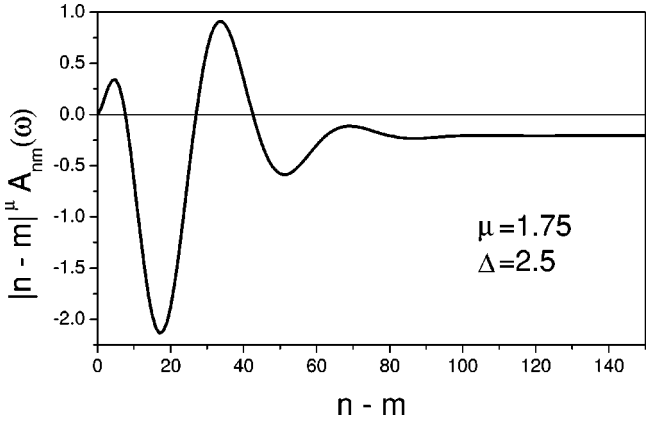

FIG. 7. Detection of the power-law component in the real-space spectral density. For the indicated parameters the CPA self-energy at $\omega=3.57$ was found to be $\sigma\approx 0.66-0.42i$. The large-distance saturation value of the plotted quantity ≈ -0.19 shows excellent agreement with the analytic result $(-1/\pi)\mathrm{Im}(\omega-\sigma-E_0)^{-2}$.

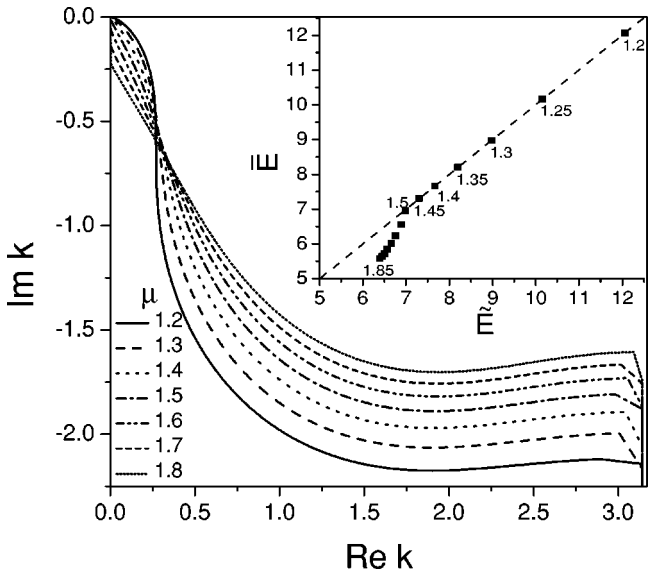

FIG. 8. Trajectories of the complex roots of the equation $\omega-\sigma(\omega)=E_k$. For the indicated values of μ, the critical energy is compared with the upper band edge (see the inset).

V. SUMMARY AND CONCLUDING REMARKS

In summary, we have investigated a tight-binding model with uncorrelated diagonal disorder and nonrandom hopping integrals given by $J_{\mathbf{nm}}=1/|\mathbf{n}-\mathbf{m}|^{\mu}$. Using the coherent-potential approximation, we calculated the density of states and the phase-coherence length related to this system. The addressed quantities were found to be affected by disorder in an essentially different way depending on whether the hopping-range exponent lies in the interval $d<\mu<3d/2$ or $\mu>3d/2$. The first of these intervals is featured by the fact that, for turned-off disorder, the infinite slope of the dispersion relation produces a tail of the density of states at the high-energy part of the spectrum. The effect of disorder, which introduces the mixing of states only within a narrow energy interval, is seriously weakened due to the small number of available states. In accordance with such qualitative argument, the tail-like part of the density of states, found in a self-consistent way, remains similar to that of the disorder-free system, apart for a small uniform shift induced by disorder. For $\mu<3d/2$ the zero broadening at the edge of the tail was shown to result in the divergence of the phase-coherence length, while for $\mu>3d/2$ it remained finite across the band. Irrespectively of μ, the real-space propagator was demonstrated to contain a component decaying with coordinate as $1/|\mathbf{n}-\mathbf{m}|^{\mu}$.

The model studied in the present paper is applicable to various materials in which the energy of one-particle excitations is of dipolar origin. As an example, let us mention dipolar Frenkel excitons on two-dimensional regular lattices where molecules are subjected to randomness due to a disordered environment.[16] Some biological light-harvesting antenna systems[17] as well as dendrimers[18] may represent a realization of this model. The form of dipolar interactions dictates the value of the hopping exponent, $\mu=3$. For this value of μ, $d=2$ was shown to be the marginal case at which one starts to observe the divergence of the PCL at the upper band edge. Increasing the PCL for Frenkel excitons could be deduced after measurement of the linear absorption spectra, which in this case should fit the power-law form (19). This opens the feasibility to test our predictions from experiments at low temperature.

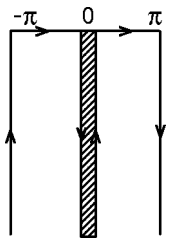

FIG. 9. Complex-momentum integration contour for $n-m<0$. The contour corresponding to $n-m>0$ is obtained by mirror reflection with respect to the horizontal axis.

ACKNOWLEDGMENTS

We are grateful to G. C. La Rocca and V. M. Agranovich for helpful discussions. D.B.B. acknowledges Universidad Complutense for hospitality. V.A.M. acknowledges support from NATO during the initial stage of this work. Work in Pisa was supported by MIUR (Grant No. PRIN-2001). Work in Madrid was supported by DGI-MCyT (Grant No. MAT2003-01533).

APPENDIX: EVALUATION OF THE REAL-SPACE PROPAGATOR (1D SYSTEM)

In this appendix, we calculate the real-space propagator for $d=1$ to show that the presence of LRH makes it vary in space nonexponentially. Following Ref. 19, we compute

$$G_{nm}(\omega)=\int_{-\pi}^{\pi}\frac{dk}{2\pi}\frac{e^{ik(n-m)}}{\omega-\sigma-E_k} \tag{A1}$$

by extending the integration contour in the complex momentum plane as illustrated in Fig. 9. The nth term in Eq. (2), decreasing not rapidly enough for $n\to\infty$, renders E_k a multivalued function of the complex k: for all integers s, branch cuts appear connecting points $2\pi s$ with $2\pi s\pm i\infty$. Integral (A1) can be split into a part due to poles and one due to the branch cuts of the integrand:

$$\begin{aligned}G_{nm}(\omega)=&-i\left(\frac{dE_k}{dk}\right)^{-1}_{k(\omega)}e^{-ik(\omega)|n-m|}\\&-i\int_0^{+\infty}\frac{d\kappa}{2\pi}e^{-\kappa|n-m|}\left[\frac{1}{\omega-\sigma-E_{i\kappa-0}}\right.\\&\left.-\frac{1}{\omega-\sigma-E_{i\kappa+0}}\right].\end{aligned} \tag{A2}$$

The first term, in which pole $k(\omega)$ is to be obtained from equation $\omega-\sigma(\omega)=E_k$ ($|\mathrm{Re}\ k|<\pi, \mathrm{Im}k<0$), falls off as an

exponential of coordinate. This behavior is similar to that observed for a full real-space propagator in the case of SRH. We show now that in the presence of LRH, the second term decays as a power of distance. In the limit of $|n-m|\to+\infty$ the upper cutoff of the integral entering Eq. (A2) can be replaced with $1/|n-m|\to 0$. Hence, only few terms in the expansion of $E_{i\kappa\pm 0}$ around $\kappa=0$ are sufficient to know large-$|n-m|$ asymptotic. The 1D version of Eq. (3) reads $E_k=2\zeta(\mu)+\Gamma(1-\mu)[(ik)^{\mu-1}+(-ik)^{\mu-1}]$, where ζ and Γ are the Riemann Zeta function and Gamma function, respectively.[20] After some algebra we get

$$G_{nm}(\omega)\sim\frac{1}{[\omega-\sigma(\omega)-E_0]^2}\frac{1}{|n-m|^{\mu}}, \tag{A3}$$

where $E_0=2\zeta(\mu)$ is the disorder-free upper band-edge energy.

*Electronic address: d.balagurov@sns.it

[1] P.W. Anderson, Phys. Rev. **109**, 1492 (1958).

[2] E. Abrahams, P.W. Anderson, D.C. Licciardello, and V. Ramakrishnan, Phys. Rev. Lett. **42**, 673 (1979).

[3] N.F. Mott and W.D. Twose, Adv. Phys. **10**, 107 (1961); B. Kramer and A. MacKinnon, Rep. Prog. Phys. **56**, 1469 (1993).

[4] J.C. Cressoni and M.L. Lyra, Physica A **256**, 18 (1998).

[5] A. Rodríguez, V.A. Malyshev, and F. Domínguez-Adame, J. Phys. A **33**, L161 (2000).

[6] A. Rodríguez, V.A. Malyshev, G. Sierra, M.A. Martín-Delgado, J. Rodríguez-Laguna, and F. Domínguez-Adame, Phys. Rev. Lett. **90**, 027404 (2003).

[7] S.-J. Xiong and G.-P. Zhang, Phys. Rev. B **68**, 174201 (2003).

[8] P. Soven, Phys. Rev. **156**, 809 (1967); D.V. Taylor, *ibid.* **156**, 1017 (1967).

[9] C. Yeung and Y. Oono, Europhys. Lett. **4**, 1061 (1987).

[10] R.J. Elliott, J.A. Krumhansl, and P.L. Leath, Rev. Mod. Phys. **46**, 465 (1974).

[11] A. Boukahil and D.L. Huber, J. Lumin. **45**, 13 (1990); M. Schreiber and Y. Toyozawa, J. Phys. Soc. Jpn. **51**, 1528 (1982); H. Fidder, J. Knoester, and D.A. Wiersma, J. Chem. Phys. **95**, 7880 (1991); L.D. Bakalis and J. Knoester, J. Lumin. **86-87**, 66 (2000).

[12] V.A. Malyshev, Opt. Spektrosk. **71**, 873 (1991) [Opt. Spectrosc. **71**, 505 (1991)]; J. Lumin. **55**, 225 (1993); V. Malyshev and P. Moreno, Phys. Rev. B **51**, 14 587 (1995); V.A. Malyshev, A. Rodríguez, and F. Domínguez-Adame, *ibid.* **60**, 14 140 (1999); V.A. Malyshev and F. Domínguez-Adame, Chem. Phys. Lett. **313**, 255 (1999); A.V. Malyshev and V.A. Malyshev, Phys. Rev. B **63**, 195111 (2001).

[13] A.A. Abrikosov, L.P. Gorkov, and I.E. Dzyaloshinski, *Methods of Quantum Field Theory in Statistical Physics* (Dover, New York, 1975)

[14] E.W. Knapp, Chem. Phys. **85**, 73 (1984).

[15] B. Velicky, S. Kirkpatrick, and H. Ehrenreich, Phys. Rev. **175**, 747 (1968).

[16] A. Nabetani, A. Tamioka, H. Tamaru, and K. Miyano, J. Chem. Phys. **102**, 5109 (1995); A. Tamioka and K. Miyano, Phys. Rev. B **54**, 2963 (1996); F. Domínguez-Adame, V.A. Malyshev, and A. Rodríguez, J. Chem. Phys. **112**, 3023 (2000); L.D. Bakalis, I. Rubtsov, and J. Knoester, *ibid.* **117**, 5393 (2002); S.S. Lampoura, C. Spitz, S. Dahne, J. Knoester, and K. Duppen, J. Phys. Chem. B **106**, 3103 (2002).

[17] H. van Amerongen, L. Valkunas, and R. van Grondelle, *Photosynthetic Excitons* (World Scientific, Singapore, 2000); T. Renger, V. May, and O. Kühn, Phys. Rep. **343**, 137 (2001).

[18] R. Kopelman, M. Shortreed, Z.-Y. Shi, W. Tan, Z. Xu, J. Moore, A. Bar-Haim, and J. Klafter, Phys. Rev. Lett. **78**, 1239 (1997); K. Herigaya, Phys. Chem. Chem. Phys. **1**, 1687 (1999); M.A. Martín-Delgado, J. Rodríguez-Laguna, and G. Sierra, Phys. Rev. B **65**, 155116 (2002); O.P. Varnavski, J.C. Ostrowski, L. Sukhomlinova, R.J. Twieg, G.C. Bazan, and T. Goodson III, J. Am. Chem. Soc. **124**, 1736 (2002).

[19] D.B. Balagurov, G.C. La Rocca, and V.M. Agranovich, Phys. Rev. B **68**, 045418 (2003).

[20] To derive this formula one can notice that $E_k=\mathrm{Li}_{\mu}(e^{ik})+\mathrm{Li}_{\mu}(e^{-ik})$, where Li is Polylogarithm, and then use the expansion presented at http://functions.wolfram.com/10.08.06.0024.01